Numerical simulation of tide-induced transport of heterogeneous sediments in the English Channel

Nicolas Guillou, Georges Chapalain

Numerical simulation of tide-induced transport of heterogeneous sediments in the English Channel

N. Guillou*[,a], G. Chapalain[a]

[a] *Laboratoire de Génie Côtier et Environnement, DELCE, CETMEF, 155 rue Pierre Bouguer Technopôle Brest-Iroise - BP 5 - 29280 Plouzané, France*

Abstract

The three-dimensional numerical model COHERENS (COupled Hydrodynamical-Ecolo -gical model for REgioNal and Shelf seas) has been adapted to compute the rates of transport as bedload and suspended load of heterogeneous bottom sediments induced by the dominant M_2 tide in the English Channel. A pre-processing of an extensive surficial sediments dataset has been performed to determine the seabed composition (grain-size distribution or presence of rocks) at the computational grid nodes. Maximum bedload and suspended load transport rates over the tidal cycle, as well as the contributions of the 10 different sedimentary classes to the mean transports are computed. Highest sediment transport rates occur in fine sediments areas located in the surroundings of high shear stresses areas. Medium sand ($d_4 = 350$ μm) is found to be predominant in bedload, while suspension load implies mainly silts ($d_1 = 25$ μm) in the inner shoreface and both fine and medium sands ($d_3 = 150$ μm, $d_4 = 350$ μm) in the outer shoreface. The offshore residual bedload transport pathways are orientated westerly in the western part of the Channel and easterly in the eastern part defining a "parting" zone which runs from the Isle of Wight to the Cotentin Peninsula. An offshore "bedload convergence" occurs in the southwest of the Dover Strait; a narrow transport pathway bypassing it along the French coastline. These features reproduce those predicted by Grochowski et al. [1993a] and provide higher resolution features like inshore headland-induced gyres, particularly along the English coastline. The new predicted general pattern of residual suspended load transport is very similar to the bedload pattern. Differences arise in the central "divergence" zone which exhibits a "Y" shape with two branches ending on both sides of the Isle of Wight, in the Baie de Seine characterized by a central "convergence" and along the English coastline studded with many headland-induced recirculations.

Key words: numerical modelling, tide, bedload, suspension load, heterogeneous sediments, English Channel.

*Corresponding author

Email addresses: nicolas.guillou@developpement-durable.gouv.fr (N. Guillou), georges.chapalain@developpement-durable.gouv.fr (G. Chapalain)

1. Introduction

The English Channel, narrow arm of the Atlantic ocean tapering eastward to its junction with the North Sea at the Dover Strait, is an active tidal shelf environment with elevation ranges as large as 13 m and current amplitudes exceeding 2 m s^{-1} between Southampton and Cherbourg [Service Hydrographique et Océanographique de la Marine , 1973]. This environment is occasionally subjected to wind-generated surface gravity waves and swell. Nevertheless, under "normal" wave conditions, near-bottom water motions and related sediment movements in water depths greater than a few meters appear mainly controlled by tidal currents [Draper, 1967; Dyer, 1986; Grochowski and Collins, 1994].

The spatial distribution of bottom sediments is highly heterogeneous with very fine sands, silts and muddy sediments in bays and estuaries (e.g., Lyme Bay, Baie de Seine) and pebbles in the Dover Strait, off the "Pays de Caux", off Brittany and over an extensive zone in the Central Channel between the Isle of Wight and the Cotentin Peninsula that divides the western Channel where bioclastic material between 0.5 and 2.5 mm and gravels abound from the eastern Channel where gravelly sand and sand of 0.15 to 0.5 mm predominate [Vaslet et al., 1979; Larsonneur et al., 1982, Fig. 1]. Rocky seabeds are found mainly off Brittany, the Cotentin Peninsula (Channel Islands Gulf) and the Cape Gris Nez. Residual bedload transport pathways deduced from morphological (asymmetry of bedforms) and sedimentological observations [e.g., Kenyon and Stride, 1970; Stride et al., 1972; Hamilton, 1979; Johnson et al., 1982] comprise an irregular "S" shaped "bedload parting" zone over the section between the Isle of Wight and the Cotentin Peninsula, and a "bedload convergence" zone between Hastings and the Baie de Somme (Fig. 2).

Numerous bi-dimensional horizontal (2DH) and three-dimensional (3D) numerical models have been set up to understand tide-induced hydrodynamics, namely the distributions of free-surface elevations, harmonic components, instantaneous and residual currents over the northwest European shelf and the nested English Channel [Pingree and

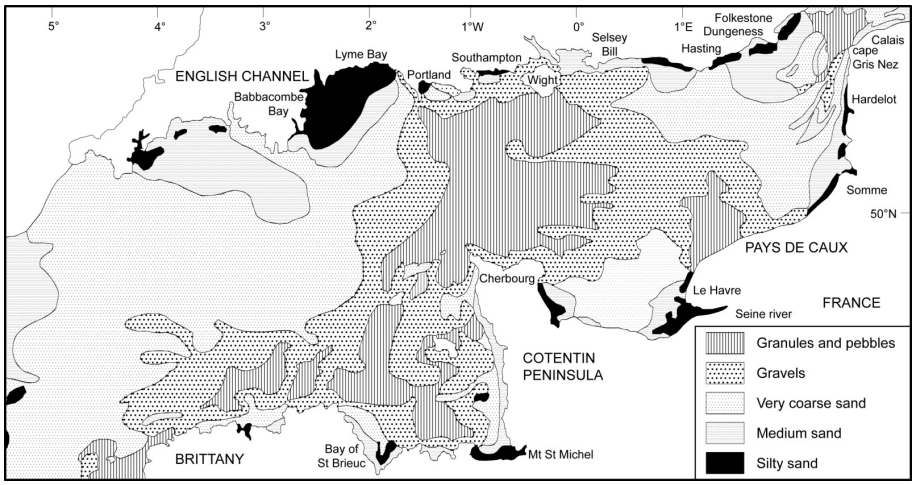

Figure 1: Schematic distribution of surficial sediment deposits in the English Channel [in Larsonneur et al., 1982].

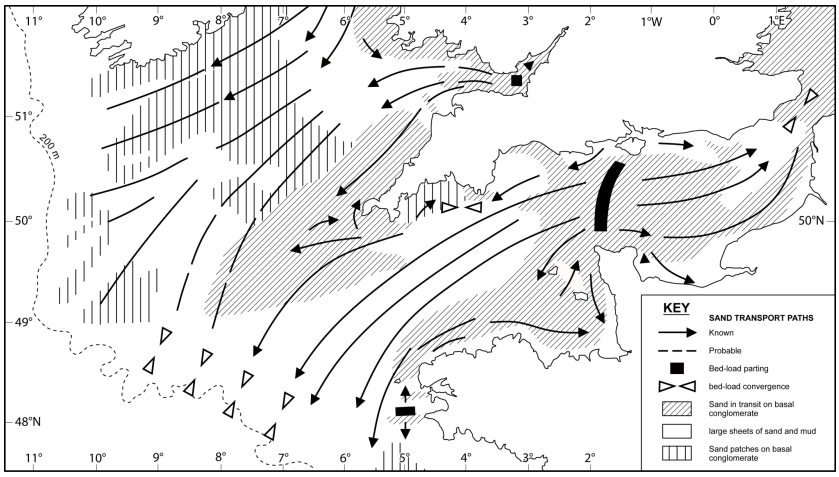

Figure 2: Transport paths for sand in the English Channel based on geomorphological and sedimentological indicators [Hamilton, 1979].

Maddock, 1977; Le Provost and Fornerino, 1985; Werner and Lynch, 1987, 1989; Lynch and Werner, 1991; Salomon and Breton, 1991a; Prandle et al., 1993; Werner, 1995]. Wind effects on the residual tide-induced circulation have been investigated by Salomon and Breton [1991b] and Perianez and Reguera [1999].

This kind of hydrodynamic models has been used to examine the advective and dispersive processes leading to the observed spatial distribution of radionuclides (125Sb, 99Tc and 137Cs) released from Cape of La Hague nuclear plant [e.g., Salomon and Breton, 1991a]. Pingree and Griffiths [1979] were the first to apply such models to investigate sediment-transport pathways by relating them to the direction of the maximum tidal bed stress. More recently, this qualitative approach was followed to study the influence of sea-level reduction over the Holocene period [Hall and Davies, 2004].

Grochowski et al. [1993a] have combined outputs from the 2DH hydrodynamic model implemented by Salomon and Breton [1991a,b] with various empirical formulae to estimate sediment bedload and total load transport rates and directions. This off-line computing approach assumes:
(i) a single granulometric mode of sedimentary particles for each specific bottom sediment stratum distinguished by Vaslet et al. [1979] excepted within gravel deposits where a second mode of medium sand (median grain-size diameter $D_{50} = 350$ μm) is added to examine its potential capability to be transported;
(ii) values of the seabed roughness parameter z_0 issued from observations published in the literature for the different encountered types of bottom sediments;
(iii) rippled sandy seabeds with a constant value of $z_0 = 0.6$ cm;
(iv) a vertical logarithmic velocity profile through the water column which results from ignoring the effect of the Coriolis force and yields colinear local depth-averaged velocity, near-bed velocity and bottom shear stress;
(v) the Engelund and Hansen's (1972) total sediment transport rate formula meaning also a global suspended load transport without any vertical dependence.

The general residual bedload transport pathways predicted by Grochowski et al.

[1993a] and shown in Figure 3 fit fairly well with the observed pattern (Fig. 2), even if their modelling procedure appears crudely correct for computing bedload sediment transport which remains highly controlled by local processes. Indeed, under typical friction velocity $u_* = 1\,\mathrm{cm\,s^{-1}}$ in the English Channel, when computing the bedload velocity U_b taken equal to $U_b = 4.8u_*$ by Nielsen [1992], the excursion of sedimentary particles transported as bedload during a tidal cycle is of the order of a few tens of meters. Nevertheless, improvements could consist in incorporating heterogeneous bottom sediments and their impacts in terms of class by class availability for transport and more subtile hiding-exposure effects. Concerning suspended load, such an off-line approach has been applied by Velegrakis et al. [1999] and Lafite et al. [2000] to estimate sediments fluxes through the Wight-Cotentin section and the Dover Strait on the basis of local measurement. Nevertheless, such a vertically integrated approach suffers more severe restrictions on account of the vertical variability of current and mixing and the horizontal excursion of suspended particles exceeding commonly a few kilometers during the tidal cycle in the study area.

The purpose of the present study is to investigate more precisely with the help of a 3D model the transportation as bedload and suspended load of sedimentary particles issued from realistic heterogeneous seabeds in the tide-dominated environment of the English Channel. A fully multicomponent sedimentary approach is suggested. To be concordant with most of the previous works and particularly those undertaken by Grochowski et al. [1993a], the model is driven by the M_2 tide and its secondary M_4 wave. The paper is organised as follows. In Section 2, the hydrodynamic and sediment transport model is first described. Some details about the spatial interpolation method used for determining the bottom sediment composition and related frictional parameters (roughness height k_b, sand ripples geometry) at the computational grid nodes are then given. In Section 3, the modelling procedure is applied to the English Channel. Maximum bedload and suspended load transport rates and mean class by class contributions during a tidal cycle are first displayed. Residual bedload and suspended load transport averaged over a tidal cycle are then derived and their pathways are discussed. Finally, conclusions and perspectives

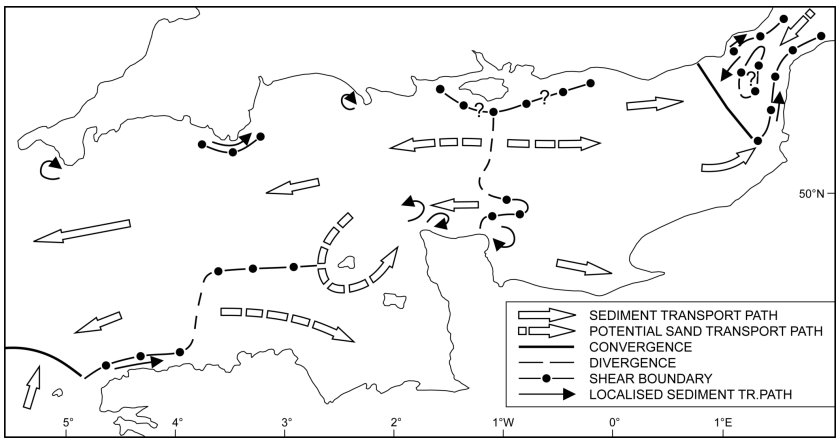

Figure 3: General pattern of bedload movement in the English Channel predicted by Grochowski et al. [1993a].

are drawn in Section 4.

2. Materials and methods

The modelling procedure is based on the hydrodynamic kernel of the 3D model COHERENS (COupled Hydrodynamical-Ecological model for REgioNal and Shelf seas) [Luyten et al., 1999a] supplemented by two sediment transport modules, the first one for bedload, the second one for suspended load. A pre-processing module aims at computing at all the computational grid nodes the seabed composition; namely the grain-size distribution for movable beds or the occurrence of rigid rocky subtrate, and derived position parameters D_p which are the grain size diameters for which p % by weight are finer (e.g., D_{16}, D_{50} or median grain-size diameter, D_{84}, D_{90}).

2.1. Model description

2.1.1. Assumptions

The flow is assumed to be turbulent over a rough bottom characterized by the roughness parameter $z_0 = k_b/30$ defined as the height above the bottom at which the fluid velocity is zero. Sandy beds with median diameter $D_{50} < 800$ μm [Soulsby, 1997] are expected to develop ripples with a height $\eta_r = 100 D_{50}$ and a wavelength $\lambda_r = 1000 D_{50}$ [Yalin, 1985]. The associated roughness parameter is given by the semi-empirical Wooding et al.'s (1973) relationship $z_0 = 2\eta_r(\eta_r/\lambda_r)^{1.4}$. Seabeds made of coarser sediments (i.e., $D_{50} \geq 800$ μm) remain featureless with a roughness parameter $z_0 = D_{90}/10$ [Van Rijn, 1993]. The parameters D_{50} and D_{90} are computed according to the grain-size distribution of bottom sediments whose modification towards the present condition are neglected.

The sedimentary particle assemblage is treated as a number N_p of discrete grain-size classes. Individual particles are assumed to be spherical with a grain-size diameter d_i ($1 \leq i \leq N_p$), non-cohesive and made of quartz with density $\rho_s = 2650\,\mathrm{kg\,m^{-3}}$. Carbonates particles which may represent up to 20 % [Vaslet et al., 1979] in some areas are assumed to be transported in a manner similar to quartz particles; the consequence of their slightly higher density (2700 to 2950 $\mathrm{kg\,m^{-3}}$) on their setlling velocity being compensated by their rounder shape due to chemical weathering.

Two modes of sediment transportation are considered: bedload and suspended load. They are linked and continuous at their transition. As mentioned by Van Rijn [1989], the first difficulty arises in determining this transition level which corresponds to the upper level of the bedload layer and the bottom level for the suspension. For a perfectly flat bed flow, Van Rijn [1984] estimated it as the maximum saltation height as 10 times D_{50}. Unfortunately, due to complex near-bed high-concentrations-induced processes (namely, hindered settling effect and turbulence damping), Van Rijn [1989] noticed that the application of a reference concentration at this level is inaccurate and not very attractive. In the case of rippled beds, the problem begining by the determination of the transtition level is even more complex. As a consequence, simple approaches with separate empirical or semi-empirical formulae for the transition level and associated reference suspended concentration and bedload formulae are recommended and thus adopted hereafter.

The suspended load is assumed to have a Newtonian behaviour. This assumption requires that the smallest length scale of the turbulence is large in comparison with the

largest particle size [Barenblatt, 1953]. For a typical friction velocity $u \simeq 10^{-2}$ m s^{-1} in the English Channel, the dissipation rate is of order $\varepsilon \sim 2\ 10^{-6}$m^{2}s^{-3}, which corresponds to a Kolmogorov microscale of turbulence $l_\kappa \sim 800\ \mu$m. This can be safely considered as large compared with the largest particles likely to move in suspension under average tidal conditions. It is also supposed that the suspension concentration is high enough to represent a continuum, but low enough to neglect particle interactions (< 8 g l^{-1}) [Lumley, 1978]. It is further assumed that the inertia of the sedimentary particles is small [Soo, 1967; Lumley, 1978], so that except for a systematic constant settling velocity w_{si} given for each grain-size class by the Soulsby's (1997) formulation, the particles follow the mean flow. According to the Soulsby and Wainwright's (1987) criterion, stratification due to suspended sediments is insignificant under typical conditions encountered in the study area. The water-sediment mixture is thus assumed homogeneous with a density $\rho = 1025$ kg m^{-3} of clear water with a temperature $T = 10$ °C and a salinity $S = 35$ psu, practical salinity units.

2.1.2. Model formulations

The hydrodynamic kernel of COHERENS solves the continuity equation and the Reynolds-averaged momentum equations derivated using the Boussinesq's (1823, 1903) approximations. The hydrostatic equilibrium is applied on the vertical. The horizontal eddy viscosity ν_H is parametrized following Smagorinsky [1963]. The vertical eddy viscosity is expressed as $\nu_T = 0.108k^2/\varepsilon$ where k is the turbulent kinetic energy and ε is its dissipation rate. These turbulent moments are obtained by solving a pair of transport equations which are well-known as the $k-\varepsilon$ turbulence closure scheme [e.g., Launder and Spalding, 1974; Rodi, 1984]. The momentum and turbulent equations are subjected to bottom boundary conditions derived from the law of wall. The set of equations is expressed in a spherical-σ coordinate system. Further details are available in Luyten et al. [1999a].

The instantaneous volumetric suspended sediment concentration C_i of each grain-size class subscripted i, with $1 \leq i \leq N_p$, satisfies the transport equation

$$\frac{\partial HC_i}{\partial t} + \nabla.\left(HC_i\mathbf{u}\right) + \frac{\partial}{\partial\sigma}\left[\left(\tilde{w} - w_{si}\right)C_i\right] = \frac{\partial}{\partial\sigma}\left(\frac{\lambda_T}{H}\frac{\partial C_i}{\partial\sigma}\right) + \nabla.\left(H\lambda_H\nabla\left(C_i\right)\right) \tag{1}$$

where t denotes time, $\mathbf{u}$ is the horizontal velocity vector, H is the instantaneous total water depth, $\tilde{w}$ is the vertical velocity normal to σ-planes, $\boldsymbol{\nabla}$ is the horizontal gradient operator, λ_H is the horizontal eddy diffusivity parametrized following Smagorinsky [1963] and λ_T is the vertical eddy diffusivity expressed as $\lambda_T = 0.177k^2/\varepsilon$.

A zero mass flux condition is imposed at the free-surface. The bottom boundary condition specifies the net mass flux through the bottom level of suspension. This flux is the difference between downward advection due to settling of the particles or deposition rate D_i, and upward entrainment of sediment from the seabed E_i:

$$w_{si}C_i + \frac{\lambda_T}{H}\frac{\partial C_i}{\partial\sigma} = D_i - E_i \tag{2}$$

The deposition rate is simply expressed as

$$D_i = w_{si}C_i^{bot} \tag{3}$$

where C_i^{bot} is the near-bed suspended sediment concentration (SCC) [e.g., Lick, 1982; Lavelle et al., 1984; Chapalain and Thais, 2000].

The method used here to specify the entrainment rate E_i follows Van Rijn [1986], Celik and Rodi [1988, 1991] and Chapalain and Thais [2000]. It is based on the physical hypothesis that the flow always entrains as much sediment from the seabed as it can with the energy available. This implies that, for a situation with a loose bed of unlimited sediment material supply, the entrainment always occurs as its maximum rate. This entrainment rate of sediment class i under full capacity equilibrium situation (i.e., zero net flux across the bottom corresponding to a balance between deposition and entrainment) is

$$E_i = w_{si} C_i^{ref}. \tag{4}$$

The maximum equilibrium near-bed reference SSC C_i^{ref} is given by the semi-empirical expression of Smith and Lean [1977]

$$C_i^{ref} = f_i C_b \left(\frac{\gamma_0 T_{si}}{1 + \gamma_0 T_{si}} \right) \tag{5}$$

where f_i is the availability of sediment in size class i, taken equal to the percentage of bed sediments in this class and $C_b = 0.65$ is the total volume concentration of sediment in the settled bed (1 - porosity). The SSC computations are performed with a resuspension parameter $\gamma_0 = 5.5 \times 10^4$ found to give a good agreement between predicted and measured total SSC 5 m above the bottom at an experimental site off Hardelot beach in the south of Boulogne-sur-Mer in the eastern English Channel [Guillou, 2007; Guillou et al., 2009]. Notice that this value falls in the range $\left[10^{-5}; 10^{-3}\right]$ obtained by compiling values found by Dyer [1980], Wiberg and Smith [1983], Drake and Cacchione [1989] and Vincent and Green [1990] in continental shelf seas. The local normalized excess skin shear-stress for class i is defined as

$$T_{si} = \mathrm{Max}\left(\frac{\tau_{skin} - \xi_i \tau_{cri}}{\xi_i \tau_{cri}}, 0 \right) \tag{6}$$

where τ_{skin} is the module of the skin bottom shear stress, τ_{cri} is the critical value above which sediment particles of class i are moved given by the Soulsby and Whitehouse's (1997) formulation and ξ_i is an empirical hiding-exposure factor.

On featureless seabeds, τ_{skin} is equal to the overall bottom shear stress $\tau_b = \rho u_{*b}^2$. On rippled beds, the skin shear stress represents only a part of the overall shear stress averaged over a ripple wavelength τ_b which also includes the form drag. Following Li [1994], its module is expressed as

$$\tau_{skin} = \tau_b \left[\alpha \left(\frac{u_{*b}}{\eta_r} \right) + \beta \right]^2 \tag{7}$$

with

$$(\alpha, \beta) = \begin{cases} (0.125\ \mathrm{s}, 0.373) & \text{for } u_{*b}/\eta_r < 2.3\ \mathrm{s}^{-1} \\ (0.107\ \mathrm{s}, 0.266) & \text{for } u_{*b}/\eta_r \geq 2.3\ \mathrm{s}^{-1}. \end{cases} \tag{8}$$

The empirical hiding-exposure factor ξ_i is here given by the Day's (1980) relationship

$$\xi_i = 0.4 \sqrt{1.6 \frac{D_{50}}{d_i}} \frac{1}{\sigma_g^{0.28}} + 0.6 \tag{9}$$

with $\sigma_g = \sqrt{D_{84}/D_{16}}$. This expression yields for a heterogeneous sediment a lessened erosion rate of small hidden grains $\xi_i > 1$ and an enhancement of erosion rate of coarse exposed grains $\xi_i < 1$ when compared with a single class sediment.

The vertically-integrated instantaneous cumulative suspended sediment transport rate is computed as

$$\mathbf{Q}_s = \sum_i^{N_p} \mathbf{Q}_{si} = \sum_i^{N_p} \left[\int_{z_a}^{H} C_i \mathbf{u} dz \right] \tag{10}$$

where z_a is the bottom level of the suspension given by Smith and Lean [1977].

Here, the instantaneous cumulative bedload transport is simply expressed following Van Rijn [1984] as

$$\mathbf{Q}_b = \sum_i^{N_p} \mathbf{Q}_{ci} = 0.053 \sum_i^{N_p} \left[f_i \sqrt{g d_i^3 (s-1)} D_{*i}^{-0.3} T_{si}^{2.1} \right] \mathbf{n} \tag{11}$$

where $\mathbf{n}$ is the unit vector having the same direction as the near-bed horizontal velocity vector at the first vertical grid cell above the bottom and

$$D_{*i} = \left[\frac{(s-1)g}{\nu^2} \right]^{1/3} d_i \tag{12}$$

is the dimensionless grain size in which appears the molecular viscosity ν of sea water at 10 °C and 35 psu equal to 1.36×10^{-6} m^2 s^{-1}, the acceleration due to gravity g and the relative sediment density $s = \rho_s/\rho$.

The residual bedload and suspended transport vectors are computed by summing the instantaneous bedload and suspended load transport vectors (Eqs. 10-11) over a tidal cycle, respectively.

2.1.3. Numerical resolution

The barotropic (external) and the baroclinic (internal) modes of hydrodynamic and SSC transport equations obtained with an explicit mode-splitting are discretized on a regular staggered grid by numerical schemes for space and time issued from the standard COHERENS code [Luyten et al., 1999a]. Only two modifications in connection with the open boundary conditions and the near bottom resolution have been implemented. The first modification consists in (i) imposing the normal depth-averaged and local horizontal velocity components with the help of the implicit Blumberg and Kantha's (1985) condition and the straightforward Blumberg and Mellor's (1987) radiation condition, respectively, and (ii) zero tangential horizontal velocity components. The second modification is the implementation of a near-bed refined computational grid with 7 regular σ-levels nested between the standard bottom and the first vertical σ-COHERENS grid point in order to improve the computation of SSC and deposition rates near and at the water-sediment interface. On this nested grid, the velocity and the viscosity are prescribed analytically according to the law of wall solutions. In contrast, SSC equations are numerically solved through the entire water column, from the lower nested grid point to the upper grid point near the free-surface in order to avoid matching problems particularly tedious during deposition phases around slack waters. Further details on this topic are available in Guillou [2007] and Guillou et al. [2009].

2.2. Seabed composition pre-processing

The availability f_i of sedimentary particles from each class i appearing in Equations 5 and 11, as well as the parameters η_r, λ_r and z_0 depending on the derived positions parameters D_{16}, D_{50}, D_{84}, D_{90} are determined at each grid node by applying a spatial interpolation method to an observed grain size distribution dataset. On account of the multivariable feature of this type of data, the statistical spatial interpolation approach proposed by Leprêtre et al. [2006] is adopted. The different steps of this approach which combines a Spherical Factorial Analysis (SFA) and krigings are summarized in Figure 4. For more details, refer to Leprêtre et al. [2006].

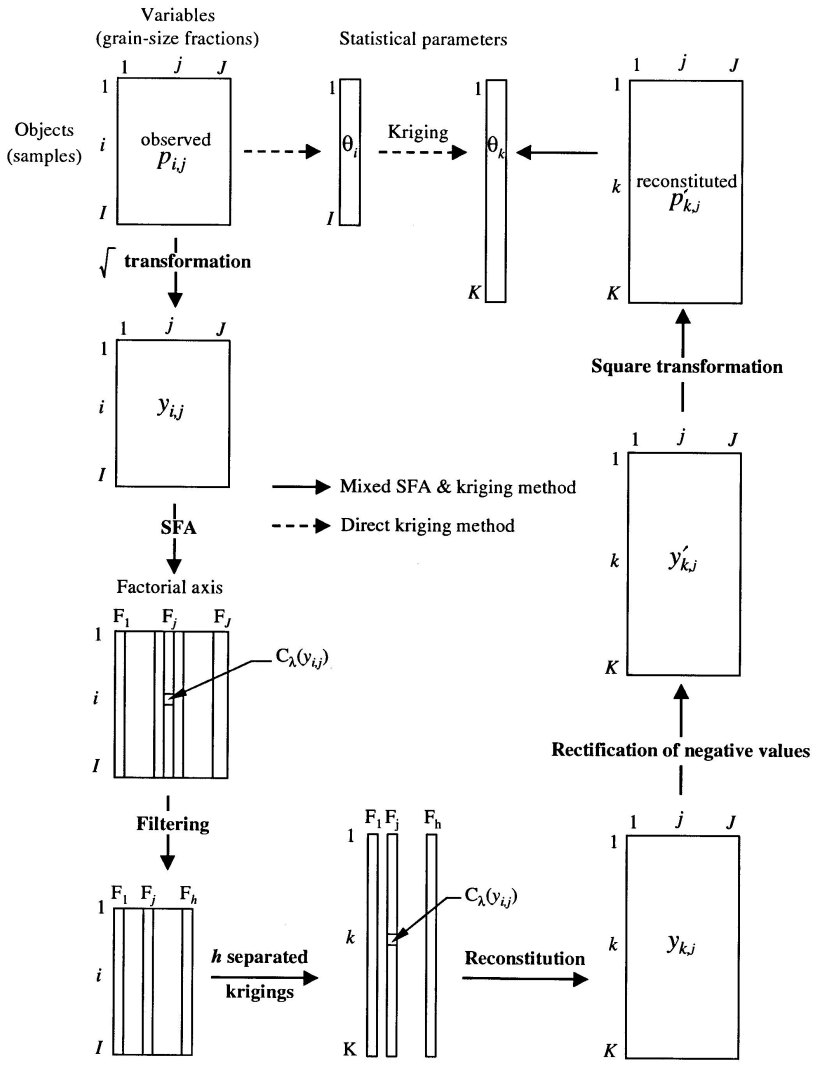

Figure 4: Flow chart of the mixed SFA-kriging spatial interpolation method [after Leprêtre et al., 2006].

3. Application and discussion

3.1. Model setup

The geographical domain for full computation of hydrodynamics and sedimentary processes extends in longitude from 3 °300 W to 3 °000 E and in latitude from 48 °410 N to 51 °300 N (Fig. 5). It is discretized on a 142 × 108 horizontal grid with a spacing of 3 km and an 11 uniform vertical σ-grid cells supplemented with the near-bed 7-σ-levels sublayer. Time steps for the external and internal modes are 30 and 300 s, respectively. In order to achieve more suitable open boundary conditions, the computational domain is extended to a larger domain from 4 °000 W to 4 °692 E and in latitude from 48 °410 N to 52 °837 N for hydrodynamic computations. The computational grid spacing and time steps are conserved, but the near-bed sublayer nested grid is ignored. The additional bottom roughness is set to an uniform value of $z_0 = 0.0035$ m [Luyten et al., 1999b; Guillou et al., 2009].

As mentioned before, the model is driven by the English Channel dominant M_2 tidal wave and its nonlinearly-generated harmonic component M_4 obtained from a long-term run of COHERENS 2DH model of the North-West European continental shelf (José Ozer, Management Unit of the North Sea Mathematical Models, personal communication, 1999). The tidal signal predicted every 10 minutes at 15 points along each open boundary is interpolated at all grid points and every time step using a cubic spline algorithm. The spin-up of the tidal forcing is set to 10 hours.

The statistical mixed SFA-Kriging interpolation method is applied to a series of 2318 bottom sediment samples which were collected from 1971 to 1976 in the framework of the "RCP 378 Benthos de la Manche" program [Cabioch et al., 1977] (Fig. 6) and passed through a series of 9 standard AFNOR sieves ranging from 50 μm to 2 cm. The 10

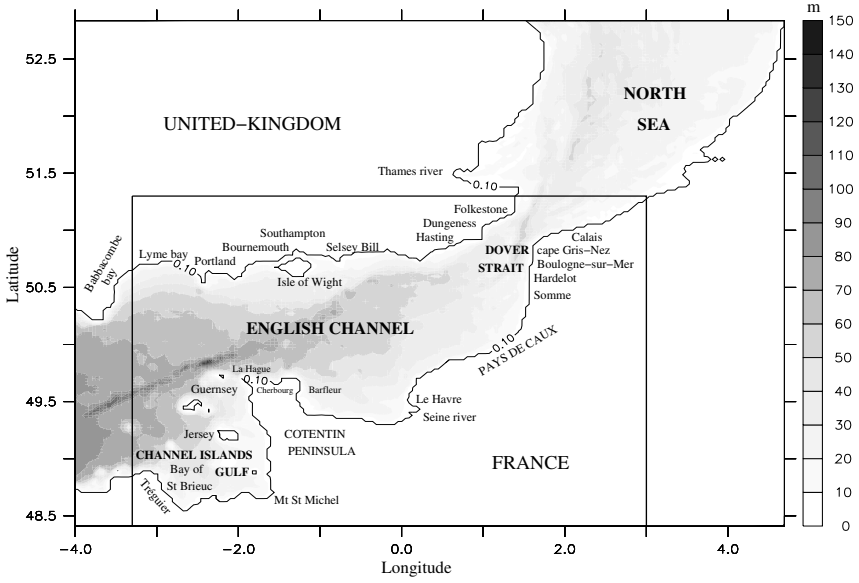

Figure 5: Bathymetry and computational domains.

corresponding classes are supplemented by a virtual class between 5.5 cm and 50 cm to account for boulders and rock outcrops (Table 1). The SFA step shows that 93 % of the total variance is accounted for by the first five axes. These major axes are only retained for the kriging step and the subsequent reconstitution steps.

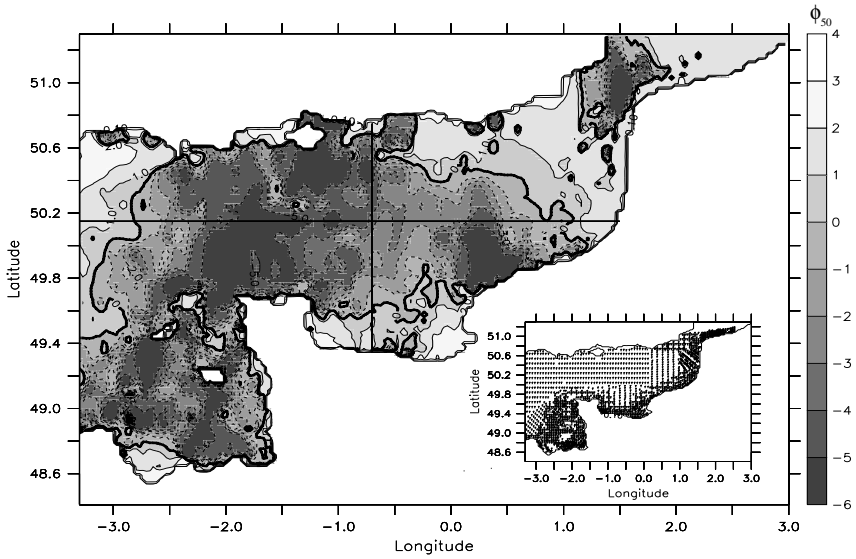

Figure 6: Interpolated median sieve diameter expressed in $\phi_{50} = \log_2(D_{50})$ (with D_{50} in mm) in the English Channel. The right-bottom sheet represents the geographic locations of the 2318 "RCP 378 Benthos de la Manche" surficial sediment samples. Black areas account for rocky outcrops.

Type of sediment fraction considered	Standard sieves diameters	Nominal grain size diameters
silt	$0 - 50$ μm	$d_1 = 25$ μm
very fine sand	$50 - 100$ μm	$d_2 = 75$ μm
fine sand	$100 - 200$ μm	$d_3 = 150$ μm
medium sand	$200 - 500$ μm	$d_4 = 350$ μm
coarse sand	$0.5 - 1$ mm	$d_5 = 750$ μm
very coarse sand	$1 - 2$ mm	$d_6 = 1.5$ mm
gravel	$2 - 5$ mm	$d_7 = 3.5$ mm
	$0.5 - 1$ cm	$d_8 = 7.5$ mm
	$1 - 2$ cm	$d_9 = 1.5$ cm
pebble	$2 - 5.5$ cm	$d_{10} = 3.75$ cm
rock outcrop	$5.5 - 50$ cm	$d_{11} = 27.75$ cm

Table 1: Grain-size diameters of each class considered.

3.2. Seabed composition versus skin friction

Figure 6 depicts the spatial distribution of interpolated median grain-size of seabed sediments at the grid nodes. This map fits fairly well with the sediment pattern established by sedimentologists [e.g., Vaslet et al., 1979; Larsonneur et al., 1982] (see Fig. 1). This agreement is particularly noticeable for the sharp sedimentary transitions in the borders of gravels-dominated areas in the central part of the English Channel and the Dover Strait, as well as for the isolated small-scale (of the order of 10 km) deposits of sands off Tréguier, Barfleur, Portland, Selsey Bill, in the north of Jersey and Guernsey and in the central English Channel between the Isle of Wight and the Cotentin Peninsula. The efficiency of the SFA-kriging method over a direct kriging of measured values is showed in Figure 7 along two orthogonal transects crossing at the point of coordinates 0 °700 W; 50 °150 N. Figure 8 depicts the spatial distributions of the fractions of silty to fine sands, medium to very coarse sands, gravels, and finally granules and pebbles.

Stride [1963], Kenyon and Stride [1970] and Stride et al. [1972] proposed a causal relationship between surficial sediments deposits and the tidal current strength. This finding was summarized by Johnson et al. [1982]. It can be precised by introducing the spatial distribution of the maximum (over the tidal cycle) skin friction velocity u_{*skin} related to the tractive force τ_{skin} acting on sea-bed materials by $u_{*skin} = \sqrt{\tau_{skin}/\rho}$ (Fig. 9). Over areas of skin shear stress τ_{skin} exceeding 2.6 $\mathrm{N\,m^{-2}}$ ($u_{*skin} > 5$ $\mathrm{cm\,s^{-1}}$) encountered in the Channel Islands Gulf, the central cross-section between the Isle of Wight and the Cotentin Peninsula, the offshore extend of the "Pays de Caux" and the central Dover Strait, granules and pebbles deposits form the bottom. Localized sources of medium to very coarse sands, between 20 to 40 %, however exist over these large areas as a consequence of a potential trapping associated with as various causes as recirculation, "convergence" of transport or substrate depression. In bays and estuaries where τ_{skin} stands below 0.10 $\mathrm{N\,m^{-2}}$ ($u_{skin} < 1$ $\mathrm{cm\,s^{-1}}$), fine sediments ($d_i < 200$ μm) predominate

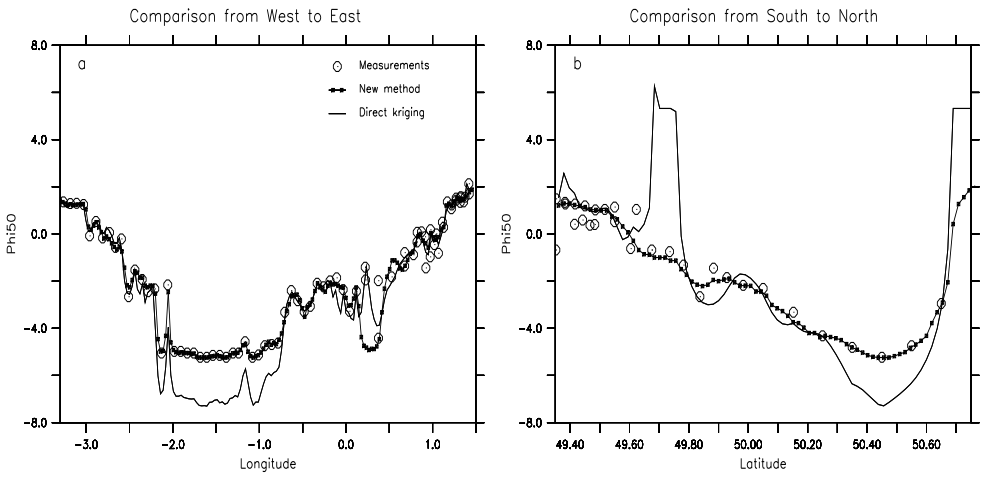

Figure 7: Comparison of median sieve diameters computed by the mixed SFA-kriging method and direct kriging method with the nearest sample observed, along (a) longitudinal and (b) latitudinal oriented lines crossing at the geographical point of coordinates 0 °700 W; 50 °150 N (Fig. 6).

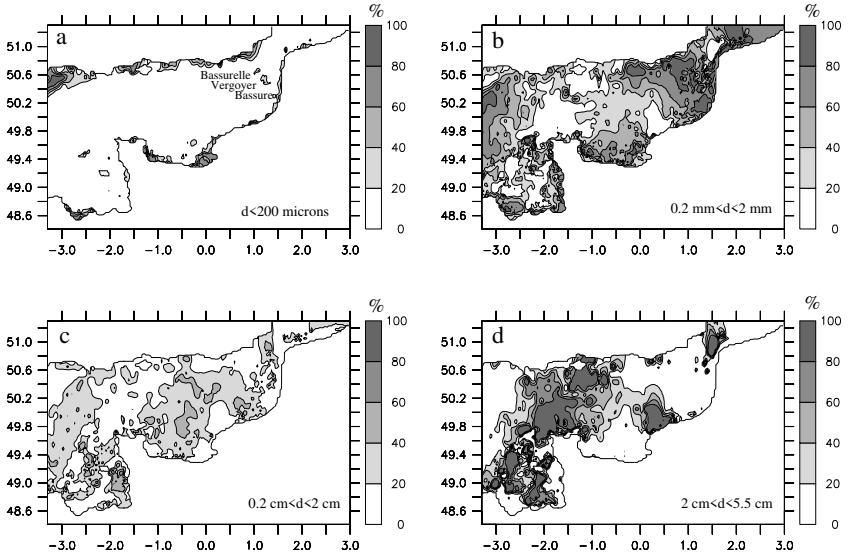

Figure 8: Predicted disponibility of bottom sediments, expressed in mass percentages, for (a) silty to fine sands, (b) medium to very coarse sands, (c) gravels and (d) granules and pebbles.

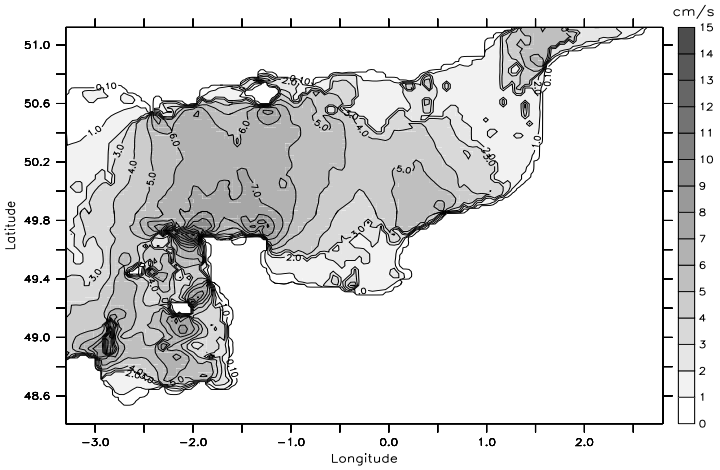

Figure 9: Predicted maximum skin friction velocity $u_{*skin} = \sqrt{\tau_{skin}/\rho}$ over a tidal cycle.

with an average disponibility of 80 %.

3.3. Maximum sediment transport rates

Figures 10 and 11 portray the maximum cumulative bedload and suspended load transport rates over a tidal cycle, respectively. Significant transports with averaged values of the maximum bedload rates of 0.6 $\mathrm{g\,cm^{-1}\,s^{-1}}$ and the suspended load rates of about 5 $\mathrm{g\,cm^{-1}\,s^{-1}}$ occur in the central part of the English Channel and the Dover Strait, where the maximum friction velocity u_{*skin} exceeds 4 $\mathrm{cm\,s^{-1}}$ and outside areas of granules and pebbles deposits. Small-scale spots of high bedload and suspended load transports reaching 5 and 40 $\mathrm{g\,cm^{-1}\,s^{-1}}$, respectively, take place inside these active regions in direct link with the localized sources of fine sands mentioned above. Elsewhere, where $u_{*skin} <$ 4 $\mathrm{cm\,s^{-1}}$, the maximum bedload and suspended load transport rates remains below 0.1 and 1 $\mathrm{g\,cm^{-1}\,s^{-1}}$, respectively. Bedload transport is found to dominate on seabeds made of very coarse sand encountered in the south of Bournemouth, off La Hague and in the northwestern Dover Strait. Conversely, suspended load transport prevails over finer bottom sediments off Portland, Selsey Bill and Wissant, north of Jersey and in the nearshore northern extend of the Isle of Wight.

The contributions of the different granulometric classes to the mean cumulative bedload and suspended load transport rates over a tidal cycle are displayed in Figures 12 and 13. 60 % of the total bedload in the English Channel concerns medium sands (0.2 mm $< d_i <$ 0.5 mm). This is consitent with the choice made by Grochowski et al. [1993b] in their bedload transport modelling to consider a sand of 250 μm in diameter. Coarser sands (0.5 mm $< d_i <$ 2 mm) contribute to the bedload over high shear stresses areas. Fine sands ($d_i <$ 200 μm) are prominent in the bedload in the Baie de Saint-Brieuc and the Seine estuary, as well as along a cross-channel transect between Hastings and the Baie de Somme in the southern Dover Strait. This latter area has been identified by Kenyon and Stride [1970], Hamilton [1979] and Grochowski et al. [1993a,b] as a "bedload convergence" zone between sedimentary fluxes from the eastern English Channel and the Dover Strait (Figs. 2 and 3). Only fine sediments with diameter smaller than 500 μm contribute to suspended sediment transport (Fig. 13). The suspended silt concentration ($d <$ 50 μm) represents more than 80 % of the total suspended sediment concentration (i) in waters located approximately 40 nautical miles offshore, and (ii) along the cross-channel line running from Hastings to the Baie de Somme. Medium sand (200 μm $< d_i <$ 500 μm) dominate suspension over the central cross-section between the Isle of Wight and the Cotentin Peninsula. From both sides of this area, the transport of fine sand (100 μm $< d_i <$ 200 μm) is dominant. Finally, in spite of an availability almost as large as the one of silts, very fine sand (50 μm $< d_i <$ 100 μm) are found to be transported in suspension only in some nearshore areas. This might be attributed to higher settling rate.

3.4. Predicted residual sediment transport pathways

The predicted tidally-averaged cumulative bedload transport vectors and the schematic pattern of bedload movement are shown in Figure 14. These predictions are in general agreement with both observations by Kenyon and Stride [1970], Stride et al. [1972], Hamilton [1979] and Johnson et al. [1982] (Fig. 2) and predictions made by Grochowski et al. [1993a,b] (Fig. 3). The large-scale residual pattern comprising the "bedload parting" zone over the central cross-section between the Isle of Wight and the Cotentin

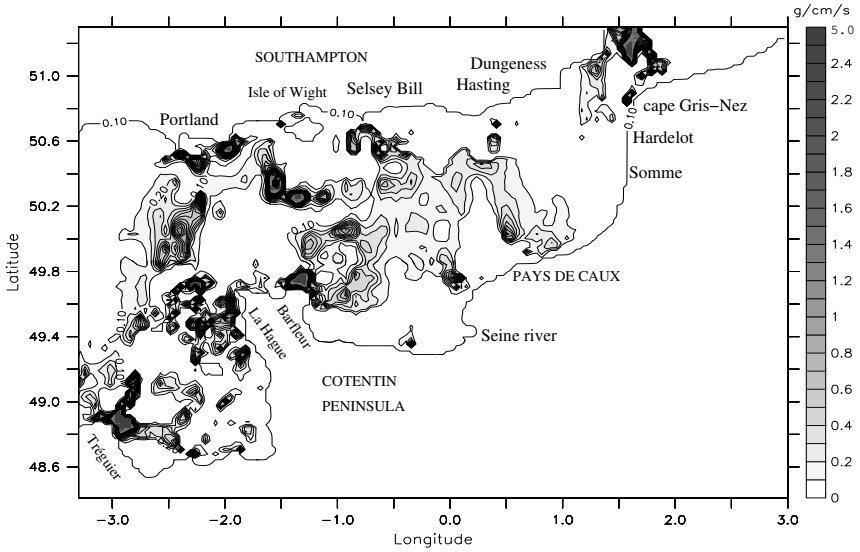

Figure 10: Predicted maximum cumulative bedload sediment transport rates over a tidal cycle.

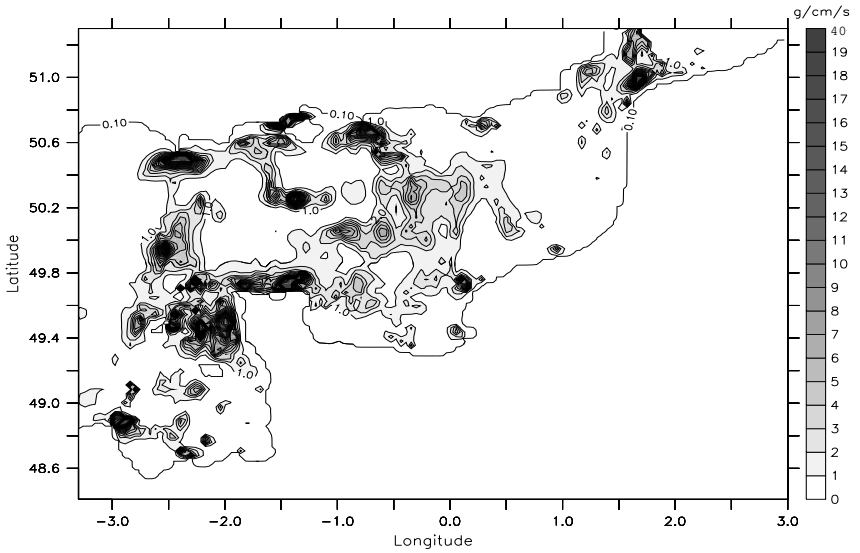

Figure 11: Predicted maximum cumulative suspended load sediment transport rates over a tidal cycle.

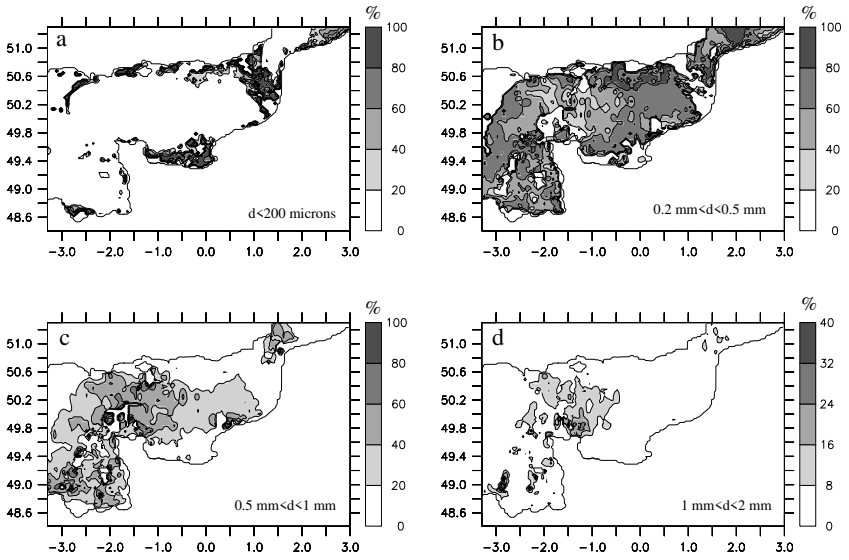

Figure 12: Percentages of (a) silty to fine sands, (b) medium sand, (c) coarse sand and (d) very coarse sand transported in mean cumulative bedload over a tidal cycle.

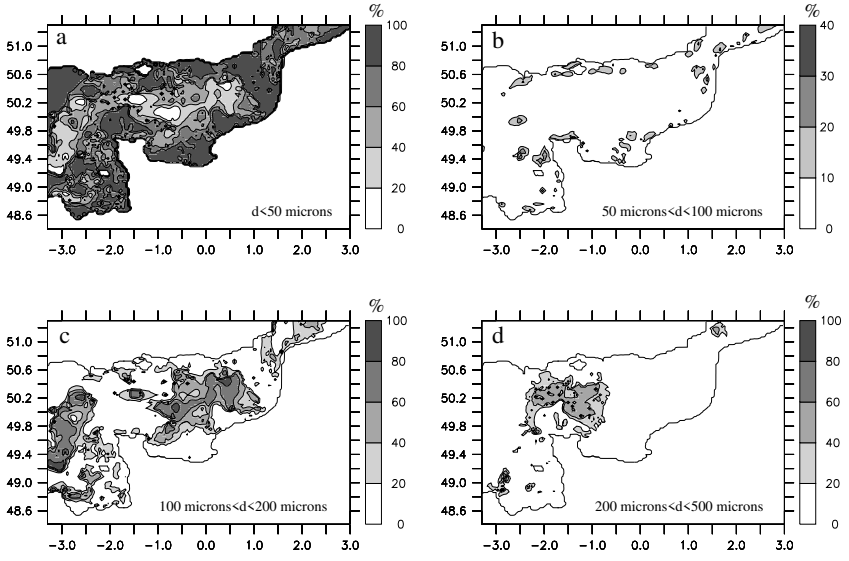

Figure 13: Percentages of (a) silty sand, (b) very fine sand, (c) fine sand and (d) medium sand transported in mean cumulative suspended load over a tidal cycle.

Peninsula and the "bedload convergence" zone along the transect joining Hastings and the Baie de Somme is well reproduced. The present fully multicomponent hydrosedimentary model confirms and predicts more precisely potential residual pathways of bedload suggested by Grochowski et al. [1993a,b] in the extensive pebbly zone present in the central Channel. The model is also found to provide better resolved small-scale features, particularly in the so-called "shear boundaries" by Grochowski et al. [1993a,b], in the northern part of the cross-section between the Isle of Wight and the Cotentin Peninsula, the Channel Islands Gulf and the central Dover Strait.

In northern part of the central divergence area, Grochowski et al. [1993a] identified two potential latitudinal sand transport paths towards the western and the eastern English Channel. These features may explain the weaker predicted bedload transport rates in the southern Isle of Wight (Fig. 10). Beyond the confirmation of the occurrence of these paths, the present model determines precisely their orientations towards SWW and SEE and the locations of their origins approximately 6 nautical miles offshore the Isle of Wight. In the east of the Isle of Wight, an anticlockwise nearshore bedload transport gyre is simulated. This feature is espected to play a role in feeding with sediment the main "bedload parting" zone as already highlighted by Grochowski et al. [1993a]. This gyre pairs with a similar anticlockwise bedload transport eddy in the east of the Selsey Bill headland.

The residual bedload circulation in the Channel Islands Gulf studded with shoals and islands is particularly complex. In this region, Grochowski et al. [1993a] defined a flood-dominated "shear boundary" lying parallel to the offshore easterly sand transport paths with a pre-eminent anticlockwise recirculation around the Guernsey island (Fig. 3). The present study reveals significant recirculations of almost 35 km in diameter around Jersey and Guernsey associated with a bedload drift towards the Mont Saint-Michel Bay with a likely consequence in terms of fullfillment as already mentioned by Ehrhold et al. [2003] on the major basis of morphological and sedimentary indicators of net bedload transport. Bedload recirculations are identified in the north of the Guernsey island, in the east of Jersey and off Tréguier. Note that the bedload recirculation in the NNW of La Hague predicted by Grochowski et al. [1993a] is not reproduced here, being replaced by an area of very low bedload transport rate ($< 10^{-6}$ g cm^{-1} s^{-1}).

In the Dover Strait, the narrow flood-dominated pathway by-passing along the French coastline the "convergence" zone running from Hastings towards the Baie de Somme exhibited by both local radioactive tracing experiments [Dewez et al., 1989; Beck et al., 1991] and Grochowski et al.'s (1993b) model is reproduced. This feature must be seen as a major contributor to sand export from the English Channel to the North Sea. Another very narrow flood-dominated path is predicted by the present model along the English coastline. The ebb-dominated path in the English waters and the central 10 km-diameter clockwise recirculation corresponding to "Le Colbart" sandbank, both pointed out by Grochowski et al. [1993b], are finally confirmed by the present study.

Figure 15 shows the predicted tidally-averaged total suspended sediment transport pathways. Similarities exist between this residual pattern and the residual bedload pattern (Fig. 14). They concern (i) the central "parting" zone between the Isle of Wight and the Cotentin Peninsula and the global associated diverging paths, (ii) the "convergence" zone along the line joining Hastings to the Baie de Somme interrupted by the flood-dominated path along the French coastline and (iii) the Channel Islands Gulf. Major differences between the two sediment patterns arise in the central "parting" zone, the

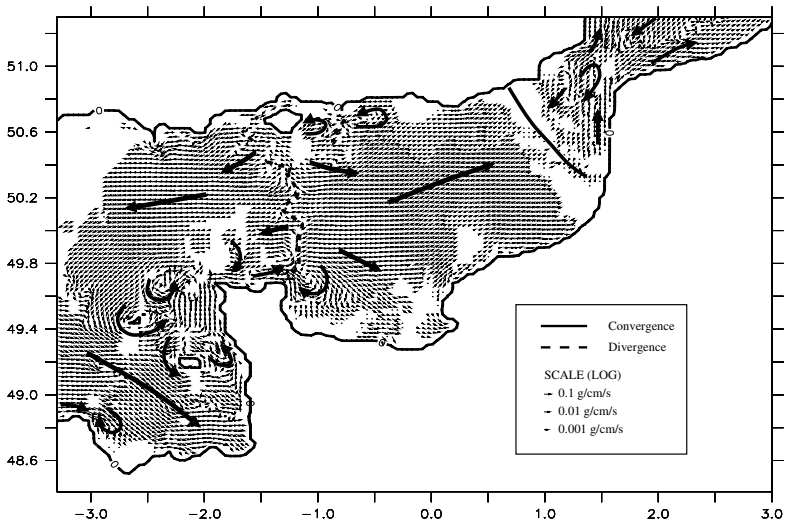

Figure 14: Predicted residual bedload transport vectors and pattern over a tidal cycle. Vectors representing bedload rates less than $10^{-6}\,\mathrm{g\,cm^{-1}\,s^{-1}}$ are not displayed.

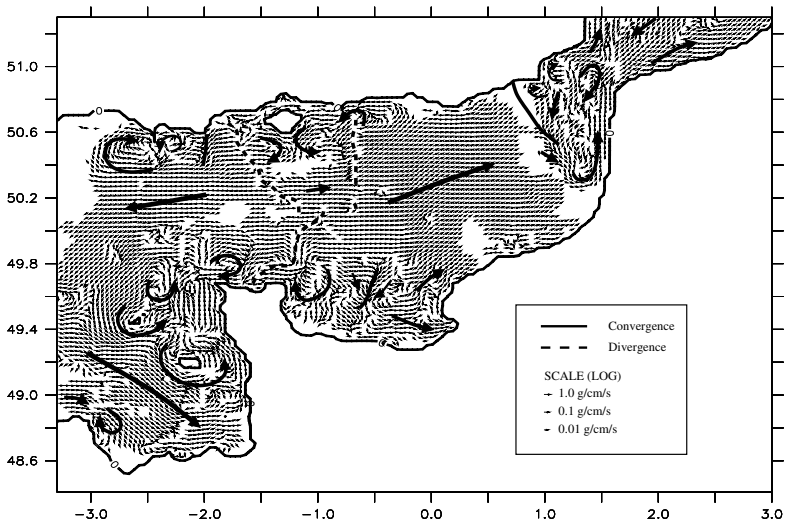

Figure 15: Predicted residual suspended load transport vectors and pattern over a tidal cycle. Vectors representing suspended rates less than $2.510^{-3}\,\mathrm{g\,cm^{-1}\,s^{-1}}$ are not displayed.

Baie de Seine and along the English coastline.

The suspended load transport "parting" zone in the central part of the Channel has a "Y" shape with a nodal point located off Bournemouth and Selsey Bill which differs from the broken "I" shape "bedload parting" zone (Fig. 14). The intermediate region between the two northern branches presents a westerly suspended sediment drift with two opposite gyres on both sides of the Isle of Wight. These features are likely responsible for trapping suspended particles. This finding is consistent with the local turbidity enhancement observed by remote sensing imaging by Menesguen and Gohin [2006].

A moderate "convergence" zone is identified in the offshore central waters of the Baie de Seine. Like the Baie du Mont Saint-Michel in the Channel Islands Gulf, this region appears as a significant sink of sediment transported in suspension.

Along the English coastline, pairs of suspended load transport gyres are found to form on both sides of the Isle of Wight and the protruding headlands of Portland Bill and Dungeness. Historically, the formation of the Shambles bank in the lee of the Portland Bill headland has been attributed to this sediment trapping feature by Pingree [1978] and Ferentinos and Collins [1980]. More recently, Bastos et al. [2002] have shown that the complex interactions between hydrodynamics, headland, bathymetry and sediments result in convergence of residual sand transport on both sides of the headland as found here.

4. Conclusions

A three-dimensional numerical model of heterogeneous sediment transport based on the hydrodynamic kernel of COHERENS code has been implemented and applied in the English Channel to investigate the bedload and suspended sediment transports induced by tidal currents. Hiding-exposure effects have been taken into account. Realistic seabed composition information consisting of granulometric distributions spatially-interpolated at the numerical grid nodes from a set of 2318 samples has been incorporated. The main outcomes of the present study are the following.

(1) Mappings of maximum total bedload and suspended load transport rates and partitioning of the mean transport rates between the different sedimentary classes are produced. The latter predictions show that maximum bedload transportation concerns dominantly medium sands ($d_4 = 350\ \mu$m) while maximum suspended load transport implies majoritarily nearshore silts ($d_1 = 25\ \mu$m).

(2) The predicted residual cumulative bedload patterns are consitent with previous results derived from morphological and sedimentological observations [e.g., Kenyon and Stride, 1970; Stride et al., 1972; Hamilton, 1979; Johnson et al., 1982] and numerical results obtained by Grochowski et al.'s (1993a) coupling the outputs of the Salomon and Breton's (1991b) 2DH hydrodynamic model and a bedload transport formula. A higher resolution of small-scales gyres on both sides of the Isle of Wight, around Jersey and Guernsey islands and the central Dover Strait is achieved.

(3) The SSC computations are found in fairly good agreement with in-situ measurements in the eastern English Channel [Guillou et al., 2009]. The innovative derived suspended transport pathways exhibit strong similarities with bedload pathways ("parting" zones over the cross-section between the Isle of Wight and the Cotentin Peninsula, "convergence" zones along the line running from Hastings towards the Baie de Somme). The

main difference arises in the schematic shape of transport patterns in the central "parting" zone: rectilinear latitudinal "I" shape for bedload against diverging latitudinal "Y" shape for suspended load. Local residual transport features are also predicted in the Baie de Seine, on both sides of the protruding headlands of Portland Bill and Dungeness.
(4) At the deca-kilometric scale, the maximum and the residual transports of sediments result from a complex interaction between the availability of sedimentary materials and transport patterns. On one hand, the amount of sediment transported as bedload and/or suspension and the associated transport rates are controlled by the availability of sedimentary particles. On the other hand, localized sources of movable sedimentary particles are controlled through an active trapping mechanism by protruding headland-induced recirculations and small-scale "convergences".

The present study is restricted to the transport of sedimentary particles issued from the bottom of the computational domain under the hydrodynamic forcing of tides. A prospective of this research will consist in incorporating meteorological forcings such as wind and induced surface gravity waves in order to estimate the impact of episodic storms on the sediment transport pathways. These further developments will aim at a better estimate of regional sediment fluxes between the eastern and western English Channel through the Wight-Cotentin cross-section and the English Channel and the southern North Sea through the Dover Strait.

Aknowledgments

The authors are grateful to Dr Louis Cabioch (Station Biologique de Roscoff) and Dr Alain Leprêtre (University of Lille) who provided the "RCP 378 Benthos de la Manche" data and to Dr José Ozer (Management Unit of the North Sea Mathematical Models, Belgium) who provided the tidal harmonic constituents issued from a long term run of COHERENS at the scale of the North-West European continental shelf. We thank Mr André Simon for improving the quality of figures. Computations were performed on computer facilities CAPARMOR (CAlcul PARallèle Mutualisé pour l'Océanographie et la Recherche). The present paper is a contribution to the CETMEF-IUEM joint research program MEMPHYS (Mesure Et Modélisation des Processus HYdrodynamiques et Sédimentaires dans les écosystèmes côtiers).

References

Barenblatt, G. T., 1953. On the motion of suspended particles in a turbulent flow. Prikladnaya Matematika i Mekhanika (Applied Mathematics and Mechanics (PMM)) 17 (3), 261–274.

Bastos, A.C., Kenyon, N.H., Collins, M.B. (2002). Sedimentary processes bedforms and facies, associated with a coastal headland: Portland Bill, Southern UK. Marine Geology 187, 235-258.

Beck, C., Clabaut, P., Dewez, S., Vicaire, O., Chamley, H., Augris, C., Hoslin, R., Caillot, A., 1991. Sand bodies and sand transport paths at the English Channel-North Sea border: morphology, dynamics and radioactive tracing. Oceanologica Acta 11, 111–121.

Blumberg, A. F., Kantha, L. H., 1985. Open boundary conditions for circulation models. Journal of Hydraulic Engineering 11, 237–255.

Blumberg, A. F., Mellor, G. L., 1987. A description of a three-dimensional coastal ocean circulation model. In: Three-Dimensional Coastal Ocean Models, Coastal and Estuarine Sciences. 4. American Geophysical Union, Washington DC, 1–16.

Boussinesq, J., 1823. Essai sur la théorie des eaux courantes. Mémoire présenté par divers savants à l'Académie des Sciences de Paris. 23. Paris, 380-398.

Boussinesq, J., 1903. Théorie analytique de la chaleur, mise en harmonie avec la thermodynamique et avec la théorie mécanique de la lumière. Gauthier-Villars, Paris.
Cabioch, L., Gentil, F., Glacon, R., Retière, C., 1977. Le macrobenthos des fonds meubles de la Manche; distribution générale et écologie. In: Biology of benthic organisms, Keegan, B.F., Ceidigh, P.O. and Caston, P.J. (Eds.), Pergamon Press, Oxford, pp. 115–128.
Celik, I., Rodi, W., 1988. Modelling suspended sediment transport in non-equilibrium situations. Journal of Hydraulic Engineering 10 (114), 1157–1119.
Celik, I., Rodi, W., 1991. Suspended sediment-transport capacity for open channel flow. Journal of Hydraulic Engineering 2 (117), 191–204.
Chapalain, G., Thais, L., 2000. Tide, turbulence and suspended sediment modelling in the Eastern English Channel. Coastal Engineering 41, 295–316.
Day, T. J., 1980. A study of the transport of graded sediments. Technical Report Number IT 190, HRS Wallingford.
Dewez, S., Clabaut, P., Vicaire, O., Beck, C., Chamley, H., Augris, C., 1989. Transits sédimentaires résultants aux confins Manche-Mer du Nord. Bulletin de la Société Géologique de France 8, 1043–1053.
Drake, D. E., Cacchione, D. A., 1989. Estimates of the suspended sediment reference concentration (c_a) and resuspension coefficient (γ_0) from near-bed observations on the California shelf. Continental Shelf Research 9, 51–64.
Draper, L., 1967. Wave activity at the sea bed around northwestern Europe. Marine Geology 5, 133–140.
Dyer, K. R., 1980. Current velocity profiles over rippled bed and the threshold of movement of sand. Estuarine Coastal Marine Science 10, 181–189.
Dyer, K. R., 1986. Coastal and estuarine sediment dynamics. John Wiler and Sons, N.Y., 342 pp.
Ehrhold, A., Guillou, S., Auffret, J. P., Garlan, T., Nguyen, K. D., 2003. Bedload transport modelisation in a bay characterized by a macrotidal environment: example of the Mont-Saint-Michel bay (Manche, France). Oceanologica Acta 26, 443–455.
Engelund, F., Hansen, E., 1972. A monograph on sediment transport in alluvial streams, 3rd edition. Technical Press, Copenhagen.
Ferentinos, G., Collins, M., 1980. Effects of shoreline irregularities on a rectilinear tidal current and their significance in sedimentation processes. Journal of Sedimentary Petrology 50 (4), 1081–1094.
Grochowski, N. T. L., Collins, M. B., 1994. Wave activity on the sea-bed of the English Channel. Journal of the Marine Biological Association of U.K. 74, 739–742.
Grochowski, N. T. L., Collins, M. B., Boxall, S. R., Salomon, J. C., 1993a. Sediment transport predictions for the English Channel, using numerical models. Journal of the Geological Society, London, 150, 683–695.
Grochowski, N. T. L., Collins, M. B., Boxall, S. R., Salomon, J. C., Breton, M., Lafite, R., 1993b. Sediment transport pathways in the eastern Channel. Oceanologica Acta 16 (5-6), 531–537.
Guillou, N., 2007. Rôles de l'hétérogénéité des sédiments de fond et des interactions houle-courant sur l'hydrodynamique et la dynamique sédimentaire en zone subtidale - applications en Manche orientale et à la pointe de la Bretagne. Ph.D. thesis, Université de Bretagne Occidentale, 469 pp.
Guillou, N., Chapalain, G., Thais, L., 2009. Three-dimensional modelling of tide-induced suspended transport of seabed multicomponent sediments in the eastern English Channel, Journal of Geophysical Research - Oceans, in press.
Hall, P., Davies, A. M., 2004. Modelling tidally induced sediment-transport paths over the northwest european shelf: the influence of sea-level reduction. Ocean Dynamics 54, 126–141.
Hamilton, D., 1979. The geology of the English Channel, South Celtic Sea and continental margin, South Western Approaches. In: The north-west European Shelf seas: the sea bed and the sea in motion. I. Geology and Sedimentology. Banner, F., Collins, M., Massie, K. (Eds.), Oceanography Series 24A. Elsevier, 61–87.
Johnson, M. A., Kenyon, N. H., Belderson, R. H., Stride, A. H., 1982. Sand transport. In: Offshore Tidal Sands. Processes and Deposits. Stride, A. (Ed.), Chapman and Hall, London, 58–94.
Kenyon, N. H., Stride, A. H., 1970. The tide-swept continental shelf sediments between the Shetland Isles and France. Sedimentology 14, 159–173.
Lafite, R., Shimwekll, S, Grochowski, N., Dupont, J.P., Nash, L., Salomon, J.C., Cabioch, L., Collins, M., Gao, S., 2000. Suspended particulate matter fluxes through the Straits of Dover, English Channel: observations and modelling. Oceanologica Acta, 23, 6, 687-699.
Larsonneur, C., Bouysse, P., Auffret, J. P., 1982. The superficial sediments of the English Channel and its western approaches. Sedimentology 29, 851–864.
Launder, B. E., Spalding, D. B., 1974. The numerical computation of turbulent flows. Computer Methods

in Applied Mechanics and Engineering 3, 269–289.
Lavelle, J. W., Mofjeld, H. O., Baker, E. T., 1984. An in situ erosion rate for fine-grained marine sediment. Journal of Geophysical Research 89, 6543–6552.
Le Provost, C., Fornerino, M., 1985. Tidal spectroscopy of the English Channel with a numerical model. Journal of Physical Oceanography, 1009–1031.
Leprêtre, A., Chapalain, G., Carpentier, P., 2006. Une méthode d'interpolation des caractéristiques granulométriques des sédiments superficiels. Bulletin de la Société Géologique de France 177 (2), 89–95.
Li, M. Z., 1994. Direct skin friction measurements and stress partitioning over moveable sand ripples. Journal of Geophysical Research C1 (99), 791–799.
Lick, W., 1982. Entrainment, deposition, and transport of fine-grained sediments in lakes. Hydrobiologia 91, 31–40.
Lumley, J. L., 1978. Two-phase and non-newtonian flows. Topics in Applied Physics, 289–324.
Luyten, P. J., Jones, J. E., Proctor, R., Tabor, A., Tett, P., Wild-Aden, K., 1999a. COHERENS: A COupled Hydrodynamics-Ecological model for REgioNal and Shelf seas - Model Description (Available on CD-ROM *via* http://www.mumm.ac.be/coherens). Management Unit of the North Sea Mathematical Models, Report MAS3-CT97-0088, Belgium, 911 pp.
Luyten, P. J., Jones, J. E., Proctor, R., Tabor, A., Tett, P., Wild-Aden, K., 1999b. COHERENS: A COupled Hydrodynamics-Ecological model for REgioNal and Shelf seas - North Sea Case Study. Management Unit of the North Sea Mathematical Models, Report MAS3-CT97-0088, Belgium, 211 pp.
Lynch, D. R., Werner, F. E., 1991. Three-dimensional velocities from a finite-element model of English Channel and southern bight tides. In: B. Parker, J. W., Sons (Eds.), Tidal Hydrodynamics. 183–200.
Menesguen, A., Gohin, F., 2006. Observation and modelling of natural retention structures in the English Channel. Journal of Marine Systems 63 (3-4), 244–256.
Nielsen, P., 1992. Coastal Bottom Boundary Layers and Sediment Transport. World Scientific Publishing, Singapore, Advanced Series on Ocean Engineering, vol. 4.
Perianez, R., Reguera, J., 1999. A numerical model to simulate the tidal dispersion of radionuclides in the English Channel. Journal of Environmental radioactivity 43 (1), 51–64.
Pingree, R. D., 1978. The formation of the Shambles and other banks by tidal stirring of the seas. Journal of the Marine Biological Association of U.K., 58, 211–226.
Pingree, R. D., Griffiths, D. K., 1979. Sand transport paths around the British Isles resulting from M_2 and M_4 tidal interactions. Journal of the Marine Biological Association of UK 59, 497–513.
Pingree, R. D., Maddock, L., 1977. Tidal residuals in the English Channel. Journal of the Marine Biological Association of UK 57, 339–354.
Prandle, D., Loch, S. G., Player, R., 1993. Tidal flow through the Straits of Dover. Journal of Physical Oceanography 23, 23–37.
Rodi, W., 1984. Turbulence models and their application in hydraulics. 2nd edition. International Association for Hydraulic Research, Delft, Netherlands.
Salomon, J. C., Breton, M., 1991a. Courants résiduels de marée dans la Manche. Oceanologica Acta 11, 47–53.
Salomon, J. C., Breton, M., 1991b. Fluxmanche's first results in modelling hydrodynamics through the Channel and Dover Strait. In: (FLUXMANCHE) Hydrodynamic and Biogeo-chemical fluxes in the eastern Channel; Fluxes into the North Sea. Fist Annual Progress Report, June 1990-May 1991, 9–14.
Service Hydrographique et Ocanographique de la Marine, 1973. Courants de marée de Dunkerque à Brest. Imprimerie Nationale, Paris.
Smagorinsky, J., 1963. General circulation experiments with the primitive equations, I, the basic experiments. Monthly Weather Review 91, 99–164.
Smith, J. D., Lean, S. R. M., 1977. Spatially averaged flow over a wavy surface. Journal of Geophysical Research 12 (82), 1735–1746.
Soo, S. L., 1967. Fluid Dynamics of Multiphase Systems. Blaisdell Publishing, Waltham, MA.
Soulsby, R., 1997. Dynamics of marine sands. H. R. Wallingford, 249 pp.
Soulsby, R. L., Wainwright, B. L. S. A., 1987. A criterion for the effect of suspended sediment on near bottom velocity profiles. Journal of Hydraulic Research 25 (3), 341–355.
Soulsby, R. L., Whitehouse, R. J. S. W., 1997. Thresholds of sediment motion on coastal environments. In: Proceedings Pacific Coasts and Ports '97 Conference. University of Canterbury, New Zealand, 149–54.
Stride, A. H., 1963. Current-swept sea floors near the southern half of Great Britain. Journal of the Geological Society, London 119, 175–199.

Stride, A. H., Belderson, R. H., Kenyon, N. H., 1972. Longitudinal furrows and depositional sand bodies of the English Channel. In: Colloque sur la géologie de la Manche, Mémoires du Bureau de Recherches Géologiques et Minières. 79, 233–240.

Van Rijn, L. C., 1984. Sediment transport, part I: Bedload transport. Journal of Hydraulic Division 10 (110), 1613–1641.

Van Rijn, L. C., 1986. Mathematical modelling of suspended sediment in non-uniform flows. Journal of Hydraulic Engineering, 112, 433–455.

Van Rijn, L. C., 1989. Handbook Sediment Transport by Currents and Waves - Rep. H 461. Delft Hydraulic Laboratory.

Van Rijn, L. C., 1993. Principles of Sediment Transport in Rivers, Estuaries and Coastal Seas. 6-5. Aqua Publications, Amsterdam.

Vaslet, D., Larsonneur, C., Auffret, J. P., 1979. Map of the surficial sediments of the English Channel, scale 1:500,000. Bureau de Recherches Géologiques et Minières, Orlans, France.

Velegrakis, A.F., Michel, D, Collins, M.B., Lafite, R., Oikonomou, E.K., Dupont, J.P., Huault, M.F., Lecouturier, M., Salomon, J.C., Bishop, C., 1999. Sources, sinks and resuspension of suspended particulate matter in the eastern English Channel. Continental Shelf Research, 19, 1933-1957.

Vincent, C. E., Green, O. M., 1990. Field measurements of the suspended sand concentration profiles and fluxes, and of the resuspension coefficient γ_0 over a rippled bed. Journal of Geophysical Research 95, 15591–15601.

Werner, F. E., 1995. A field test case for tidally forced flows: a review of the tidal flow forum. Coastal and Estuarine Studies 47, 269–283.

Werner, F. E., Lynch, D. R., 1987. Field verification of wave equation tidal dynamics in the English Channel and southern North Sea. Advances Water Resources 10, 115–130.

Werner, F. E., Lynch, D. R., 1989. Harmonic structure of channel/southern Bight tides from a wave equation simulation. Advances Water Resources 12, 194–203.

Wiberg, P. L., Smith, J. D., 1983. A comparison of field data and theoritical models for wave-current interactions at the bed of the continental shelf. Continental Shelf Research 2, 147–162.

Wooding, R. A., Bradley, E. F., Marshall, J. K., 1973. Drag due to regular arrays of roughness elements of varying geometry. Boundary-Layer Meteorology 5, 285–308.

Yalin, M. S., 1985. On the determination of ripple geometry. Proc. A.S.C.E., Journal of the Hydraulic Division 8 (111), 1148–1155.